

Aalborg Universitet



## Nonlinear Control of Induction Motors: A Performance Study

Rasmussen, Henrik; Vadstrup, P.; Børsting, H.

*Publication date:*  
1998

*Document Version*  
Også kaldet Forlagets PDF

[Link to publication from Aalborg University](#)

*Citation for published version (APA):*

Rasmussen, H., Vadstrup, P., & Børsting, H. (1998). *Nonlinear Control of Induction Motors: A Performance Study*.

### General rights

Copyright and moral rights for the publications made accessible in the public portal are retained by the authors and/or other copyright owners and it is a condition of accessing publications that users recognise and abide by the legal requirements associated with these rights.

- Users may download and print one copy of any publication from the public portal for the purpose of private study or research.
- You may not further distribute the material or use it for any profit-making activity or commercial gain
- You may freely distribute the URL identifying the publication in the public portal -

### Take down policy

If you believe that this document breaches copyright please contact us at [vbn@aub.aau.dk](mailto:vbn@aub.aau.dk) providing details, and we will remove access to the work immediately and investigate your claim.

# Nonlinear Control of Induction Motors: A Performance Study

H. Rasmussen

P. Vadstrup and H. Børsting

Department of Control Engineering  
Aalborg University, Fredrik Bajers Vej 7  
DK-9220 Aalborg, Denmark

Grundfos A/S  
DK-8850 Bjerringbro, Denmark

## Abstract

*A novel approach to control of induction motors, based on nonlinear state feedback has previously been presented by the authors. The resulting scheme gives a linearized input-output decoupling of the torque and the amplitude of the field. The proposed approach is used to design controllers for the field amplitude and the motor torque. The method is compared with the traditional Rotor Field Oriented Control method as regards variations in rotor resistance and magnetizing inductance.*

## NOMENCLATURE

$a$	complex spatial operator $e^{j2\pi/3}$
$i_{sA,B,C}$	stator phase currents A,B and C
$u_{sA,B,C}$	stator phase voltages A,B and C
$\bar{i}_s$	stator current complex space vector
$\bar{u}_s$	stator voltages complex space vector
$R_s, R_r$	resistances of a stator and rotor phase winding
$L_s, L_r$	self inductance of the stator and the rotor
$L_m$	magnetizing inductance
$L_{sl}, L_{rl}$	leakage inductances $(L_s - L_m), (L_r - L_m)$
$T_r$	rotor time constant ( $T_r = L_r/R_r$ )
$\sigma$	leakage factor $(1 - L_m^2/(L_s L_r))$
$R_r'$	referred rotor resistance ( $R_r' = (L_m/L_r)^2 R_r$ )
$L_s'$	referred stator inductance ( $L_s' = \sigma L_s$ )
$L_m'$	referred magnetizing inductance ( $L_m' = (1 - \sigma)L_s$ )
$p$	time derivative operator ( $p \equiv d/dt$ )
$Z_p$	number of pole pair
$\omega_{mech}$	angular speed of the rotor
$\omega_{mR}$	angular speed of the rotor flux
$i_{mR}$	rotor magnetizing current
$\rho$	rotor flux angle
$c_m$	torque factor ( $c_m = 1.5 Z_p L_m'$ )

## 1 Introduction

The development of high-performance controllers for drives using an induction motor as an actuator is shortly stated by Leonhard [7] as "30 Years Space Vectors, 20 Years Field Orientation and 10 Years Digi-

tal Signal Processing with Controlled AC-drives". The relevance of field oriented control is witnessed by a large numbers of investigations carried out both from a theoretical and a practical point of view [6]. The scheme works with a controller which approximately linearizes and decouples the relation between input and output variables by using the simplifying hypothesis that the actual motor flux is kept constant and equal to some desired value.

In the last 10 years with digital signal processing, significant advances have been made in the theory of nonlinear state feedback control [4], and particular feedback linearization and input-output decoupling techniques have been successfully applied for control of induction motor drives [8],[5],[1],[2],[9] and [10].

In De Luca [8], a simplified model is used, i.e. only the electromagnetic part is modeled assuming the speed as a slowly varying parameter. Exact decoupling in the control of electric torque and flux amplitude using the amplitude and frequency of the voltage supply as inputs is obtained by a static state feedback compensator. The resulting nonlinear feedback is quite complex due to the fact that the formulation adopted to carry out the decoupling is based on a reference frame rotating with the stator flux vector. Krzeminski [5] took advantage from the intrinsic decoupling connected with the rotor field orientation, but in his paper the decoupled system does not end up with a double integrator, but with a second order system depending on the motor parameters. Bellini [1] presents a different approach for decoupling of flux and speed, which yields a simple linearized model, constituted by two lines of double integrators, without requiring particular complex computations to determine the components of the motor supply voltage. Because of the mechanical equation for speed the load torque has to be known or estimated.

Flux and speed is also decoupled in Frick et. all. [2] and Marino et. all [9]. Marino propose an adap-

tive method but it is not obvious how limitation of the motor currents influence the method. By proposing a nonlinear controller based on a two-step input-output decoupling Frick et. all. [2] obtain precise limitation of motor currents and voltages which is indispensable in all applications demanding maximum torque production.

The method of most of the above references uses adaptation of the load torque. However this is a limiting factor to the servo performance because adaptation of the load torque is slow. In order to circumvent this problem torque and flux are decoupled in this paper assuming speed as a measured parameter.

The proposed method has previously in Rasmussen et. all. [12] been verified by experiments, and has demonstrated performance which is comparable to traditional Field Oriented Control. In this paper a comparing study is carried out between the two methods. They are compared and evaluated against variations in rotor resistance  $R_r$  and magnetizing inductance  $L_m$ , which are the two significant parameter variations in an induction motor caused by temperature and magnetic saturation.

## 2 Induction motor model

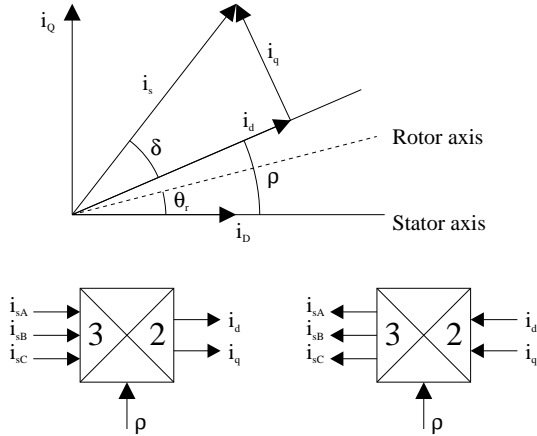


Figure 1: Definitions of transformation angles and symbols

If the currents in the stator coordinates ( $i_{sA}, i_{sB}, i_{sC}$ ) and the field angle  $\rho$  are known, then the following equations based on the angle definition given in Fig. 1 give the transformation from stator

coordinates to field coordinates

$$\bar{i}_s = \frac{2}{3}(i_{sA} + ai_{sB} + a^2i_{sC})e^{-j\rho}$$

In a reference frame fixed to the *rotor magnetizing current* we have with the angular definitions given in Fig. 1, the d-axis in the direction of the rotor magnetizing current  $i_{mR}e^{j\rho}$  and the q-axis orthogonal to the d-axis. Defining the synchronous speed  $\omega_{mR} = \frac{d\rho}{dt}$  and

$$\begin{aligned} f_1 &= (-R_s i_{sd} + \omega_{mR} L'_s i_{sq} - R'_r (i_{sd} - i_{mR}))/L'_s \\ f_2 &= (-R_s i_{sq} - \omega_{mR} L'_s i_{sd} - \omega_{mR} L'_m i_{mR})/L'_s \\ f_3 &= (i_{sd} - i_{mR})/T_r \\ f_4 &= Z_p \omega_{mech} + i_{sq}/(i_{mR} T_r) = \omega_{mR} \end{aligned}$$

the motor model is given by

$$\frac{d}{dt} \begin{Bmatrix} i_{sd} \\ i_{sq} \\ i_{mR} \\ \rho \end{Bmatrix} = \begin{Bmatrix} f_1 \\ f_2 \\ f_3 \\ f_4 \end{Bmatrix} + \begin{Bmatrix} \frac{1}{L'_s} \\ 0 \\ 0 \\ 0 \end{Bmatrix} u_{sd} + \begin{Bmatrix} 0 \\ \frac{1}{L'_s} \\ 0 \\ 0 \end{Bmatrix} u_{sq} \quad (1)$$

with the developed electrical torque given by

$$m_e = \frac{3}{2} Z_p L'_m i_{mR} i_{sq} = c_m i_{mR} i_{sq} \quad (2)$$

## 3 Nonlinear decoupling

The input-output decoupling problem is to find a state feedback such that the transformed system is input-output decoupled, i.e. one input influence one output only. Detailed information on input-output decoupling can be found in [4].

Using the definitions

$$x = \{i_{sd}, i_{sq}, i_{mR}, \rho\}^T \quad u_1 = u_{sd} \quad u_2 = u_{sq}$$

$$\begin{aligned} f_1 &= \frac{1}{L'_s} (-R_s x_1 + (Z_p \omega_{mech} + \frac{x_2}{x_3 T_r}) L'_s x_2 - R'_r (x_1 - x_3)) \\ f_2 &= \frac{1}{L'_s} (-R_s x_2 - (Z_p \omega_{mech} + \frac{x_2}{x_3 T_r}) (L'_s x_1 + L'_m x_3)) \\ f_3 &= \frac{1}{T_r} (x_1 - x_3) \\ f_4 &= Z_p \omega_{mech} + \frac{x_2}{x_3 T_r} \end{aligned}$$

$$f = \{f_1, f_2, f_3, f_4\}^T$$

$$g_1 = \{1/L'_s, 0, 0, 0\}^T$$

$$g_2 = \{0, 1/L'_s, 0, 0\}^T$$

the induction motor equations (1) are given by

$$\dot{x} = f(x) + g_1 u_1 + g_2 u_2$$

and the torque equation (2) is

$$m_e = c_m x_2 x_3$$

This system can be linearized by a state space transformation and a nonlinear state feedback, if and only if the following conditions are satisfied in an open set  $U$  of  $R^4$ , as shown by Isidori [4]

$$G_0 = \text{span}(g_1, g_2)$$

must be involutive and have constant dimension in  $U$  and

$$G_1 = \text{span}(g_1, g_2, [f, g_1], [f, g_2])$$

must have the same dimension as the state vector in  $U$ . The Lie bracket  $[f, g]$  used is defined by

$$[f, g] = \frac{\partial g}{\partial x} f - \frac{\partial f}{\partial x} g$$

For  $x_3$  not equal to zero both conditions are easily verified. It is therefore possible to find  $\dim(G_1) - \dim(G_0) = 2$  output functions allowing the linearization of the system.

The two output functions are denoted by  $y_1 = h_1(x)$  and  $y_2 = h_2(x)$ . If the two functions satisfy the conditions

$$\begin{aligned} L_{g_1} h_1(x) &= 0 \\ L_{g_1} h_2(x) &= 0 \\ L_{g_2} h_1(x) &= 0 \\ L_{g_2} h_2(x) &= 0 \end{aligned} \quad (3)$$

where  $L_h \lambda(x)$  is the Lie derivative of the function  $\lambda(x)$  along the vector field  $h(x)$ , defined by

$$L_h \lambda(x) = \sum_i \frac{\partial \lambda(x)}{\partial x_i} h_i(x)$$

Because the relative degree  $r_1$  and  $r_2$  associated with each output is greater than one the total relative degree  $r = r_1 + r_2$  is less than or equal to the degree of the state vector  $n = 4$ . The conditions (3) then lead to a total relative degree  $r = n$ . This means that no zero dynamics have to be considered. Equation (3) leads to

$$\frac{\partial h_1}{\partial x_1} = \frac{\partial h_2}{\partial x_1} = \frac{\partial h_1}{\partial x_2} = \frac{\partial h_2}{\partial x_2} = 0$$

giving output functions only depending on  $x_3$  and  $x_4$ . The two simplest functions satisfying this are  $y_1 = h_1(x_3, x_4) = x_3$  and  $y_2 = h_2(x_3, x_4) = x_4$  leading to a decoupling of the flux amplitude and the flux angle. In the field weakening region where both field amplitude and torque are varied a more interesting

result would be decoupling of torque and field amplitude. This means that candidates for output functions are

$$\begin{aligned} h_1(x) &= x_3 \\ h_2(x) &= x_2 x_3 \end{aligned}$$

if the zero dynamics of the resulting uncontrollable state is stable.

The approach to obtain the input-output linearization of the system is to take the time derivative of the output functions until the input appears.

$$\begin{aligned} \dot{y}_1 &= L_f h_1 + L_{g_1} h_1 u_1 + L_{g_2} h_1 u_2 = L_f h_1 \\ \dot{y}_1 &= L_f^2 h_1 + L_{g_1} L_f h_1 u_1 + L_{g_2} L_f h_1 u_2 \\ \dot{y}_2 &= L_f h_2 + L_{g_1} h_2 u_1 + L_{g_2} h_2 u_2 \end{aligned}$$

After some calculations the following equations are obtained for  $x_3 \neq 0$

$$\begin{aligned} \dot{y}_1 &= f_3 \\ \ddot{y}_1 &= \frac{1}{T_r L'_s} (u_1 + L'_s (f_1 - f_3)) \\ \dot{y}_2 &= \frac{x_3}{L'_s} (u_2 + L'_s (f_2 + \frac{x_2}{x_3} f_3)) \end{aligned}$$

New inputs defined by

$$\begin{aligned} \nu_1 &= \frac{1}{T_r L'_s} (u_1 + L'_s (f_1 - f_3)) \\ \nu_2 &= \frac{x_3}{L'_s} (u_2 + L'_s (f_2 + \frac{x_2}{x_3} f_3)) \end{aligned}$$

lead to the following decoupled outputs for a field amplitude different from zero

$$\begin{aligned} \ddot{y}_1 &= \nu_1 \\ \dot{y}_2 &= \nu_2 \end{aligned}$$

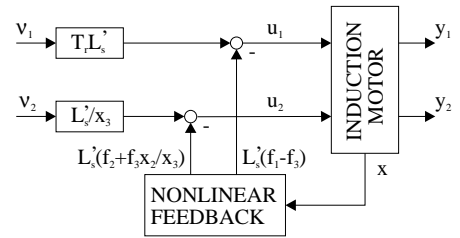


Figure 2: Nonlinear state feed-back giving two decoupled linear systems  $\ddot{y}_1 = \nu_1$  and  $\dot{y}_2 = \nu_2$

The inputs  $u_1$  and  $u_2$  are then given by the non-linear equations

$$\begin{aligned} u_1 &= T_r L'_s \nu_1 - L'_s (f_1 - f_3) \\ u_2 &= \frac{L'_s}{x_3} \nu_2 - L'_s (f_2 + \frac{x_2}{x_3} f_3) \end{aligned} \quad (4)$$

## 4 Uncontrollable dynamics

Due to the fact that the relative degree  $r = 2 + 1 < n = 4$  the input-output decoupling leaves one uncontrollable state to be analyzed for dynamic behavior. Based on the coordinates giving output decoupling the following coordinates

$$\eta = \{h_1, L_f h_1, h_2, x_4\}^T = \left\{ x_3, \frac{1}{T_r}(x_1 - x_3), x_2 x_3, x_4 \right\}^T$$

defines a diffeomorphism for  $x_3 \neq 0$  because the Jacobian

$$\frac{\partial \eta}{\partial x} = \begin{Bmatrix} 0 & 0 & 1 & 0 \\ \frac{1}{T_r} & 0 & -\frac{1}{T_r} & 0 \\ 0 & x_3 & x_2 & 0 \\ 0 & 0 & 0 & 1 \end{Bmatrix}$$

is nonsingular for  $x_3 \neq 0$ .

*The uncontrollable dynamics of a MIMO nonlinear system is the dynamics of the system when the outputs are constrained to be constant.*

Since the constraint that the outputs identically is equal to constants implies that all the derivatives of the outputs are zero we have  $\dot{y}_1 = \ddot{y}_1 = 0$  and  $\dot{y}_2 = 0$ . Because  $y_1 = h_1$ ,  $\dot{y}_1 = L_f h_1$  and  $y_2 = h_2$  we have  $\dot{\eta}_1 = \dot{\eta}_2 = \dot{\eta}_3 = 0$ .

Since  $\dot{\eta}_1 = 0$  gives  $x_3(t) = x_3^0$ ,  $\dot{\eta}_2 = 0$  gives  $x_2(t) = x_3(t) = x_3^0$  and  $\dot{\eta}_3 = 0$  leads to  $\dot{x}_2(t)x_3^0 = 0$  giving  $x_2(t) = x_2^0$  we have in the original coordinates, that when the system operates in steady state, the system states evolves on the surface  $x_2(t) = x_3(t) = x_3^0$  and  $x_2(t) = x_2^0$  with  $x_3^0 \neq 0$ .

The uncontrollable dynamics is then given by

$$\dot{\eta}_4 = Z_p \omega_{mech} + \frac{x_2^0}{x_3^0 T_r}$$

$\eta_4$  is equal to the field angle  $\rho$  which means that the uncontrollable dynamics have and desirable behavior.

## 5 Torque and field amplitude control

### 5.1 Field Amplitude Controller

The output  $y_1 = h_1(x) = x_3$  with the decoupled dynamics  $\ddot{y}_1 = \nu_1$  is controlled by the following PD-controller

$$\nu_1 = K_1(i_{mR,ref} - y_1 - K_a \dot{y}_1)$$

giving the closed loop transfer function

$$y_1 = \frac{1}{\frac{1}{K_1} p^2 + K_a p + 1} i_{mR,ref}$$

Defining  $\alpha_1$  as a design parameter and using  $K_1 = 1/(\alpha_1 T_r)^2$  and  $K_a = 2\alpha_1 T_r$  the following transfer function from  $i_{mR,ref}$  to  $i_{mR} = y_1$  is obtained

$$i_{mR} = \frac{1}{(1 + \alpha_1 T_r p)^2} i_{mR,ref}$$

Differentiation is avoided by using  $T_r \dot{y}_1 = T_r \dot{x}_3 = x_1 - x_3$  i.e. the controller for the field amplitude is given by

$$\nu_1 = K_1(i_{mR,ref} - x_3 - K_a/T_r(x_1 - x_3))$$

together with the nonlinear transformation equation (4).

### 5.2 Torque Controller

The output  $y_2 = h_2(x) = x_2 x_3$  with the decoupled dynamics  $\ddot{y}_2 = \nu_2$  is controlled by the following P-controller

$$\nu_2 = K_2 \left( \frac{1}{c_m} m_{e,ref} - y_2 \right)$$

giving the following closed loop transfer function

$$y_2 = \frac{1}{1 + p/K_2 c_m} \frac{1}{c_m} m_{e,ref}$$

Defining  $T_2$  as a design parameter and using

$$K_2 = \frac{1}{T_2}$$

the closed loop transfer function from  $m_{e,ref}$  to  $m_e = c_m y_2$  is obtained

$$m_e = \frac{1}{1 + T_2 p} m_{e,ref}$$

the controller for the torque is therefore given by

$$\nu_2 = K_2 \left( \frac{1}{c_m} m_{e,ref} - x_2 x_3 \right)$$

together with the nonlinear transformation equation (4).

The P and PD controllers for the decoupled torque and field amplitude is shown in Fig. 3 together with the nonlinear decoupling.

## 6 Simulation

In this section sensitivity against change in rotor resistance and magnetizing inductance will be analyzed based on a simulation study.

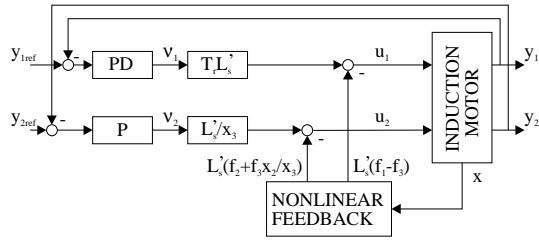


Figure 3: Decoupled torque and field amplitude control

The nonlinear control method will be compared with the traditional Rotor Field Oriented Control method with d-q current control loops.

Both methods will use the following flux estimator

$$\begin{aligned}\hat{i}_{mR}(t) &= \frac{1}{1+pT_r} i_{sd}(t) \\ \hat{\rho}(t) &= Z_p \theta_{mech} + \int_0^t \frac{i_{sq}(\tau)}{T_r \hat{i}_{mR}(\tau)} d\tau\end{aligned}$$

which is defined for  $i_{mR} \neq 0$ .

The rotor resistance  $R_r$  and the magnetizing inductance  $L_m$  change considerably due to variation in temperature and magnetic saturation. For our test motor, a GRUNDFOS 1.1 kW induction motor, these variation can be calculated.

The magnetizing inductance is minimum when the motor is unloaded. In that case the motor is very close to saturation. The magnetizing inductance is maximum when the motor torque is maximum. The minimum and maximum values for the rotor resistance is obtain for cold and hot motor respectively.

In the control systems the speed controller and field weakening function will be omitted as shown in figure 4.

The control values are given by (4) which for  $i_{mR} \neq 0$  leads to

$$\begin{aligned}\nu_1 &= \frac{1}{\alpha_1^2 T_r^2} (i_{mR,ref} - \hat{i}_{mR} - 2\alpha_1(i_{sd} - \hat{i}_{mR})) \\ \nu_2 &= \frac{1}{T_2} \left( \frac{m_{e,ref}}{c_m} - i_{sq} \hat{i}_{mR} \right) \\ u_{sd,ref} &= T_r L_s' \nu_1 + R_s i_{sd} - \omega_{mR} L_s' i_{sq} \\ &\quad + (R_r' + \frac{L_s'}{T_r})(i_{sd} - \hat{i}_{mR}) \\ u_{sq,ref} &= \frac{L_s'}{\hat{i}_{mR}} \nu_2 + R_s i_{sq} + \omega_{mR} (L_s' i_{sd} + L_m' \hat{i}_{mR}) \\ &\quad - \frac{L_s' i_{sq}}{T_r \hat{i}_{mR}} (i_{sd} - \hat{i}_{mR})\end{aligned}$$

The load is simulated as

$$J \frac{d\omega_{mech}}{dt} = m_e - f_0 \omega_{mech}$$

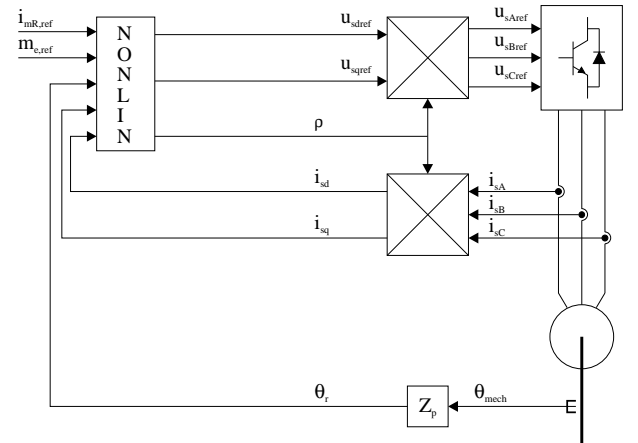


Figure 4: Field Oriented Control System with decoupling of torque and field amplitude

and the reference signals  $i_{mR,ref}$ ,  $m_{e,ref}$  are chosen as

$$i_{mR,ref} = \begin{cases} 0 & \text{for } t < 0 \\ 0.8 & \text{for } 0 \leq t < 1 \\ 0.4 & \text{for } 1 \leq t \end{cases}$$

$$m_{e,ref} = \begin{cases} 0 & \text{for } t < 0.5 \\ 0.4 & \text{for } 0.5 \leq t \end{cases}$$

The parameters used for simulation are shown in the following table

	Hot motor 100% load	Cold motor 100% load	Hot motor 200% load
$R_s[\Omega]$	9.20		
$R_r[\Omega]$	9.20	4.79	
$L_m[H]$	0.5353		0.6601
$L_{sl}[H]$	0.01228		
$L_{rl}[H]$	0.01865		
$J[kgm^2]$	0.00077		
$Z_p$	1		
$\alpha_1$	0.04		
$T_2[s]$	0.00005		

Figures 5 and 6 show the sensitivity to changes in rotor resistance and magnetizing inductance. The subfigures in the first and second column show the simulation results using the Nonlinear Decoupling Control methods and Rotor Field Oriented Control methods respectively. The dashed lines correspond to equal parameters in the motor and the model (hot motor, 100% load). The solid lines correspond to the case where motor parameters change due to temperature (cold motor) and load variations (200% load).

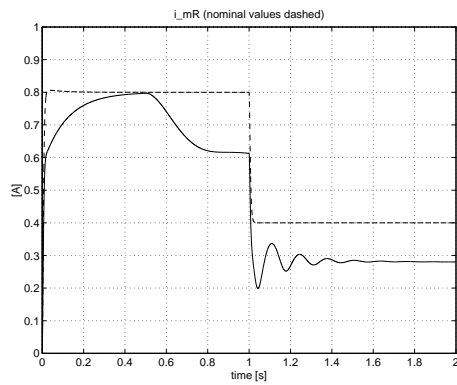
As the figures show the two methods demonstrate nearly the same dynamic behavior. Both methods are sensitive to changes in  $L_m$  and  $R_r$ . In the case of a change in  $L_m$  it would have been expected that the Rotor Field Oriented Control method would have been less sensitive due to the internal current loops.

## 7 Conclusion

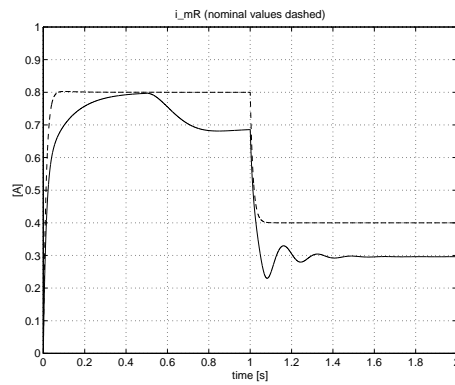
A new method based on nonlinear control theory has been compared to the traditional Rotor Field Oriented Control method. Compared to other strategies evolving from the nonlinear control theory reported in the literature this method do not need an adaptation of the motor load. Elimination of this need for adaptation implies that servo performance is present even at momentary load torque changes. Both methods are sensitive to motor parameter variations. In the case of a change in  $L_m$  it would have been expected that the Rotor Field Oriented Control method would have been less sensitive due to the internal current loops, but the simulation studies show that the two methods have nearly the same sensitivity. The nonlinear method has the advantage that it opens for a systematic way of compensating for nonlinearities like magnetic saturation effects.

## References

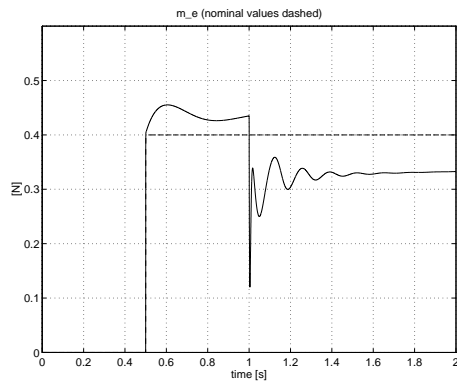
- [1] Bellini A., G. Figalli and F. Tosti. Linearized Model of Induction Motor Drives via Nonlinear State Feedback Decoupling. EPE Firenze 1991.
- [2] Frick A., E. von Westerholt and B. de Fornel. Non-Linear Control of Induction Motors via Input-Output Decoupling. ETEP Vol. 4. No. 4, July/August 1994.
- [3] Holtz J. and A.M. Khambadkone. Pulse Width Modulation for Controlled AC Motor Drives. Tutorial. EPE'93. Brighton, 1993.
- [4] Isidori A. *Nonlinear Control Systems*. Springer-Verlag Berlin (ISBN 3-540-19916-0), 1995.
- [5] Krzeminski Z. Nonlinear Control of Induction Motors. Conf.Rec. X IFAC World Congress, Vol. 3, München, 1987.
- [6] Leonhard W. *Control of Electrical Drives*. Springer Verlag Berlin (ISBN 3-540-13650-9), 1985.
- [7] Leonhard W. 30 Years Space Vectors, 20 Years Field Orientation, 10 Years Digital Signal Processing with Controlled AC-Drives. EPE Journal, vol.1, no.1, July 1991.
- [8] Luca A. De and G. Ulivi. Design of an Exact Non-linear Controller for Induction Motors. IEEE Trans. on Automatic Control, AC-34, pp. 1304-1307, 1989.
- [9] Marino R., S. Peresada and P. Valigi (1993). Adaptive input-output linearizing control of induction motors. *IEEE Tr. on Automatic Control*, vol. 38, no. 2, pp.208-221.
- [10] Ortega R. and G. Espinosa (1993). Torque regulation of induction motors. *Automatica*, vol. 29, no. 3, pp. 621-633.
- [11] H. Rasmussen. Self-tuning torque control of induction motors for high performance applications. *PhD thesis*, Department of Control Engineering, Aalborg University, Denmark, December 1995.
- [12] H. Rasmussen, P. Vadstrup and H. Børsting. Nonlinear Decoupling of Torque and Field Amplitude in an Induction Motor. FINPIE/97 Espoo Finland 1997.
- [13] Jean-Jacques Slotine and Weiping Li *Applied Nonlinear Control*. Prentice-Hall (ISBN 0-13-040049-1), 1991.



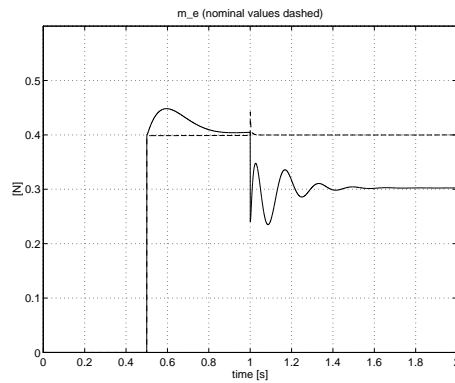
a) Magnetizing current  $i_{mR}$   
NDC



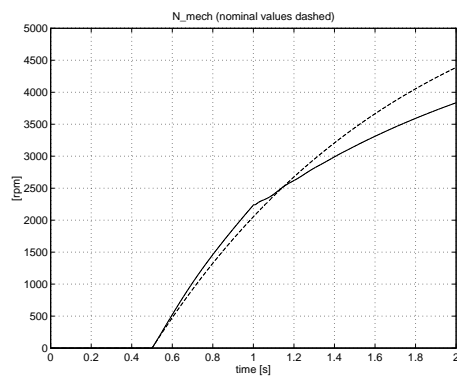
d) Magnetizing current  $i_{mR}$   
RFOC



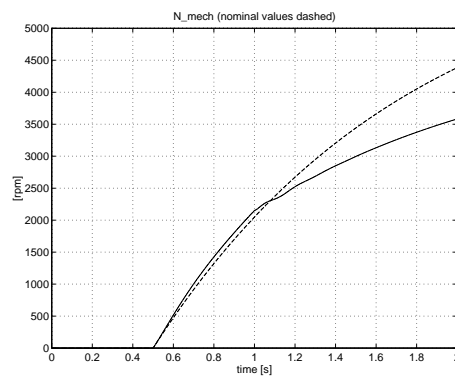
b) Developed electrical torque  $m_e$ ,  
NDC



e) Developed electrical torque  $m_e$ ,  
RFOC

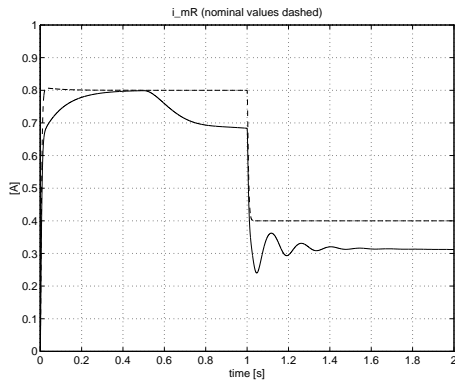


c) Rotor speed  $N_{mech}$   
NDC

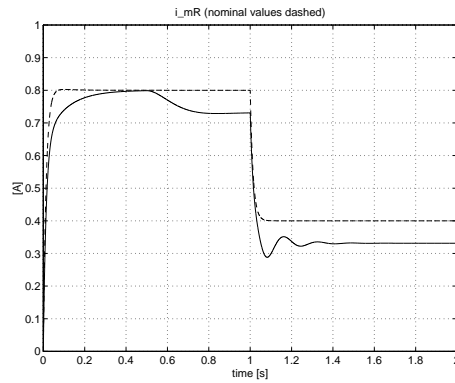


f) Rotor speed  $N_{mech}$   
RFOC

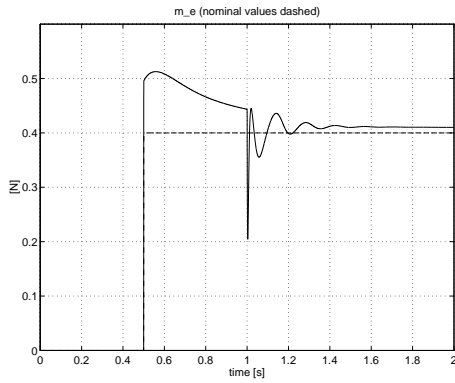
Figure 5: Sensitivity to change in rotor resistance for Nonlinear Decoupling Control (a, b and c) and Rotor Field Oriented Control (d, e and f). Dashed line (nominal motor) and solid line (cold motor)



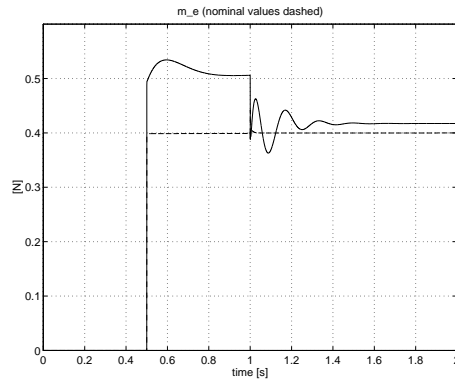
a) Magnetizing current  $i_{mR}$   
NDC



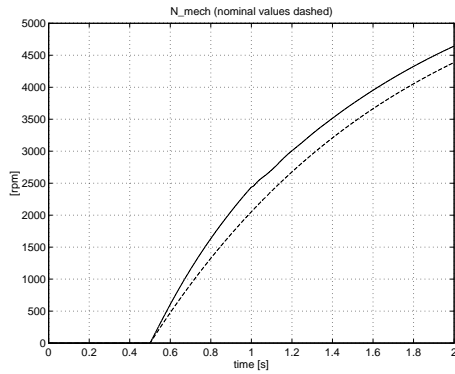
d) Magnetizing current  $i_{mR}$   
RFOC



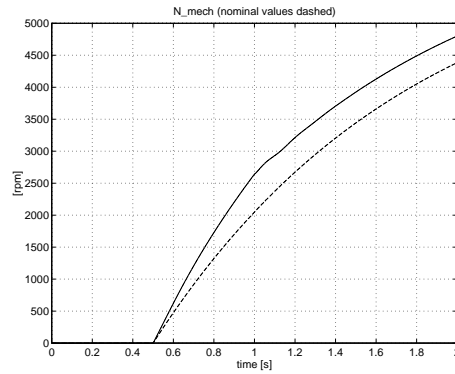
b) Developed electrical torque  $m_e$ ,  
NDC



e) Developed electrical torque  $m_e$ ,  
RFOC



c) Rotor speed  $N_{mech}$   
NDC



f) Rotor speed  $N_{mech}$   
RFOC

Figure 6: Sensitivity to change in magnetizing inductance for Nonlinear Decoupling Control (a, b and c) and Rotor Field Oriented Control (d, e and f). Dashed line (nominal motor) and solid line (200% load)